Viser Technology Pte. Ltd.
Research and Application of Materials Science
DOI: 10.33142/rams.v6i2.14587

Research Article Open Access

Ordered Mesoporous Fe-Nx/C Materials as Highly Efficient Self-supporting Electrocatalysts for Oxygen Reduction

LianYan LIAO, YuXi ZHANG, Heng Qiang ZHANG, TongYin JIN*

College of Chemistry and Chemical engineering , Hebei Minzu Normal University, Chengde, Hebei, 067000, China

*Corresponding Author: Tongyin JIN, E-mail: tyjin0521@hbun.edu.cn

Abstract

A new mesostructured non-precious-metal catalyst (NPMC) was easily created using a straightforward nanocasting technique with 1,10-phenanthroline iron chelates as the sole precursor. The resulting Fe-Nx/C material, characterized by its Hexagonal mesostructures with an ordered arrangement, Extensive surface extent, expansive pore structure, and evenly Scattered Fe-Nx groups within Graphite-like carbon structures, Established to be an remarkable self-supporting cathode catalyst for the oxygen reduction reaction (ORR). It demonstrated superior specific oxygen reduction activity in 0.1M KOH alkaline solution compared to commercial Pt/C catalysts (20wt%Pt, JM), showing a more positive onset potential (0.0V vs Ag/AgCl), approximately 1.7 times the kinetic-limiting current density of Pt-C-JM, and higher current density across the entire potential range. Additionally, it exhibited an onset potential of 0.93V (vs RHE) for ORR and about 1.3 times the current density at 0.6V (4.9mA cm^{-2}) compared to the best NPMC materials reported in the literature, with a catalyst loading of 0.6mg cm^{-2} in 0.5M H_2SO_4 media (approximately 3.8mA cm^{-2}).

Keywords: Mesoporous; Oxygen reduction reaction; non-precious metal; self-supporting catalysts

1 Introduction

Proton exchange membrane fuel cells (PEMFCs) have Inspired significant attention in the past few decades as An eco-friendly technology. A major challenge for achieving efficient electrochemical energy conversion in PEMFCs is the slow oxygen reduction reaction (ORR) that is conducted at the cathodes. To enhance the ORR rate, catalysts made from platinum or platinum-based binary (Pt-Pd) or ternary (Pt-Ru-Co) materials are typically used, as they offer the best performance for electrode reactions and long-term stability. However, the high cost and limited availability of these precious metals Inhibit the widespread commercialization of PEMFCs[1-3]. Consequently, global research efforts have focused on finding cost-effective and High-efficiency, economical non-precious metal catalysts[3-6]. While nitrogen-doped carbon nanomaterials, such as nanotubes[7-8], graphene [9-10], and mesoporous carbons[11-12], have proven to be effective catalysts due to their high electrocatalytic activity and stability for the oxygen reduction reaction (ORR) in alkaline electrolytes, their performance in acidic electrolytes is significantly lower[13-15]. Among the various non-precious metal catalysts (NPMCs) being explored as candidates to platinum-based catalysts for ORR, nitrogen-coordinated transition metals within a carbon matrix (M-Nx/C), particularly Fe-Nx/C materials[2,5], show the most promise as noble-metal-free cathode catalysts. There has been considerable focus on enhancing their active site density to improve catalytic activity through various strategies [5-6,16]. Typically, Fe-N4 chelate complexes [19] or simple precursors made from iron salts and nitrogen sources supported on carbon are used to create Fe-Nx/C catalytic materials[23-28]. However, the precursors used in the production of these traditional Fe-Nx/C catalysts often struggle to penetrate the inner pores of carbon supports, leading to active sites being primarily located on the Exterior of the carbon supports, which results in inadequate Catalytic capability for ORR[19].

An alternative approach called "ordered mesoscopic structure control" has been suggested to improve the catalytic activity of Fe-Nx/C materials for the oxygen reduction reaction (ORR) [29-31]. This method focuses on effectively concentrating active sites at the inner edges of mesoporous structures with well-organized pore channels and a high surface area by choosing suitable precursors and preparation techniques. The heating of Fe-N4 macrocycle molecules in conjunction with some kinds of carbon sources Including formaldehyde[33], sucrose[35], and the thermolysis of Ferrous acetates[34] incorporated into mesoporous CNx under inert or ammonia-containing gases, leads to the creation of effective mesoporous Fe-N-C catalytic materials[33,35]. However, the inclusion of additional carbon precursors in these processes

Received on October 7th, 2024; Accepted on November 17, 2024

reduces the fraction of reactive nitrogen species in the final products, thus complicates the even Dispersion of active nitrogen-transition metal species within the mesoporous structures[33,35]. Furthermore, Heat treatment may lead to the emergence of non-active species like Fe or FeCx and generate the unequal dispersion of carbon, nitrogen, and iron precursors, potentially obstructing catalytic active site [5]. Additionally, The mentioned mesoporous Fe-Nx/C frameworks exhibit low graphitic structures, which can optimizes surface area and active site potential but also reduce the electron conductivity of these catalysts, presenting challenges for membrane electrode assembly. The use of costly macrocycle precursors, toxic ammonia gas, and complex synthesis methods also complicates mass production and increases costs. Thus, creating highly efficient Fe-Nx/C catalytic materials for ORR using inexpensive precursors while balancing ordered mesostructures, high surface area, high active site density, and high graphitic structures remains a significant challenge.

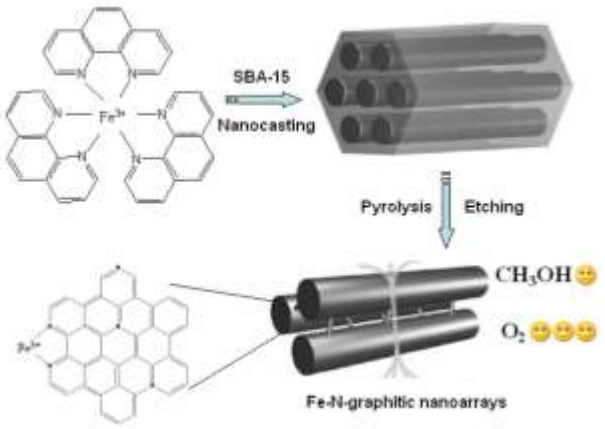

Figure 1 Synthesis of ordered mesopropus Fe-Nx/C materials as self-supporting NPMCs for ORR

In this research, we successfully synthesized ordered mesoporous Fe-Nx/C materials with desired characteristics using a standard nanocasting technique, employing Fe^{3+} phenanthroline chelates as the sole precursor (see Figure 1). Various techniques, including XRD, TEM, SEM, EDS-Mapping, BET, SAED, and XPS, confirm that the resulting materials exhibit ordered mesoporous structures, graphitic frameworks, a substantial specific surface area, and numerous active sites. The materials demonstrated highly efficient ORR catalytic activity, excellent methanol durability in electrocatalytic applications, and improved stability in both alkaline and acidic environments, demonstrated by cyclic voltammetry, current-time chronoamperometric response, and rotating-disk voltammetry measurements. Additionally, we propose potential explanations for the high activity of Fe-Nx/C materials based on the findings from electrocatalysis studies and the analysis of their active species in comparison to Fe(Co)-Nx/C, and Nx/C materials.

2 Experimental

2.1 Synthesis

In the kinetic energy theorem, students are trained to understand the relationship between kinetic energy and kinetic energy, so that students can grasp the concept of kinetic energy and gradually generate a certain concept of energy from kinetic energy. By deepening the understanding of the relationship between motion and energy, we can gradually grasp the kinetic energy theorem and learn to apply it to deal with relevant problems [2].

The goal of scientific thinking: to cultivate students' scientific thinking ability to carry out scientific experiments from the perspective of physics; Combining the analysis of experimental results with comprehensive logical reasoning to obtain conclusions; Cultivating students' ability to design experiments with scientific thinking; Through the analysis of the experimental results, the students' ability of scientific and logical reasoning, doubt and innovation is cultivated.

The objective of the experimental research is to cultivate students' ability to put forward physical problems and make scientific conjectures; Cultivating students' communication and cooperation ability through group experiments; The research is carried out by the method of controlling variables, so as to cultivate students' research thinking.

Scientific working attitude and responsibility goal: to correctly guide students to understand the relationship between kinetic energy and kinetic energy theorem and physical conditions in life, especially to let students realize that the application of kinetic energy is closely related to life, and to cultivate students' mentality of attaching importance to and loving physics. Adopt a positive attitude, train students to find problems, actively explore the concept, and cultivate students' spirit of cooperation in the search. Using kinetic energy theorem and its universal application in real life, cultivate students' sense of scientific responsibility. As the key quality of physics is an interrelated whole, it is necessary to cultivate not only students' research quality but also students' energy concept when guiding students to carry out working group research experiments; Scientific way of thinking; Scientific mentality and quality of responsibility. It can not only improve the teaching efficiency, but also enrich the teaching content.

The overall goal of classroom teaching in this competition class: Firstly, cultivate students' research quality through group experiments. Secondly, understand the concept of kinetic energy; Master the physical quantities that affect kinetic energy. Understand the application of kinetic energy expression; Let students feel the thinking process of dealing with new problems

with old knowledge through objective thinking, and learn this scientific way of thinking. Thirdly, understand the relationship between kinetic energy theorem and daily life and specific applications, so that students can feel the close relationship between physics and life and deal with problems in daily life with objective thinking.

Ordered mesoporous Fe-Nx/C materials were synthesized using three standard nanocasting methods [32], which include precursor filling, pyrolysis, and template etching. The regular preparation protocol is presented herein: 0.5g of dried SBA-15 samples, synthesized following prior publications, were combined with a 19mL alcohol solution containing 0.8g of 1,10-phenanthroline, 0.58g of $FeCl_6$ $3H_2O$ salts, and 1mL of water. The obtained mixture was stirred well, then the solvent was allowed to evaporate at ambient temperature. The derived powders were subsequently burned at about 900˚C for 120 minutes in a protective gas atmosphere, while the thermal ramp rate of 2˚C per minute initially. Finally, the products were acquired through etching the silica templates in a 20wt% HF solution for 12 hours, resulting in the formation of Fe-Nx/C.

For comparison, mesoporous cobalt-nitrogen-carbon materials (Co-Nx/C) and mesoporous nitrogen-doped carbon further synthesized by a similar preparatory technique, utilizing 0.8g of 10-phenanthroline and either 0.54g or 0g of $Co(Ac)_2$ $2H_2O$ as precursors.

2.2. Characterization

Powder X-ray diffraction patterns (XRD) were obtained using a Rigaku D/Max-2500 diffractometer operating at 40 kV and 40 mA with CuKα radiation. Transmission electron microscopy (TEM) images were captured with a JEM-2010 microscope at an acceleration voltage of 200 kV. Nitrogen adsorption and desorption measurements were conducted at 77 K using a Micromeritics Tristar 3000 analyzer. X-ray photoelectron spectroscopy (XPS) measurements were carried out on a Thermo ESCALAB 250 instrument using Al Kα radiation (1486.6 eV), with C 1s (284.6 eV) serving as a reference for binding energy correction.

2.3. Electrochemical measurment

Electrocatalytic capability of the synthesized catalysts for the oxygen reduction reaction (ORR) was assessed using cyclic voltammetry (CV) and rotating disk electrode (RDE) methods. A standard three-electrode setup was utilized, consisting of a glass carbon RDE as the working electrode, an Ag/AgCl, KCl (3 M) electrode as the reference, and a platinum wire as the counter electrode. The experiments in alkaline conditions were conducted in an O_2-saturated 0.1 M KOH solution, with the potential being cyclically scanned from -1.2 to +0.2 V at a scan rate of 10 mV/s at room temperature, following a 15-minute purging with O_2 or N_2 gas. The electrocatalytic activities for ORR in acidic conditions were explored in an O_2-saturated 0.5 M H_2SO_4 solution, with the potential scanned between 1.0 and -0.2 V (vs Ag/AgCl). The working electrode was prepared by dissolving 15 mg of mesoporous materials in 4 ml of a solvent mixture of Nafion (5%) and isopropanol (in a 1:9 volume ratio) through sonication. For comparative evaluation, a conventional catalyst consisting of 20 wt.% Pt on black carbon (JM, fuel cell grade) was also used, with a Pt-C suspension prepared using the same method. The catalyst suspension was applied to the polished glassy carbon electrode surface, which was then allowed to dry at ambient temperature before measurements, resulting in a catalyst loading of 30 μg/cm² for all working electrodes.

3. Results and Discussion

3.1 Synthesis

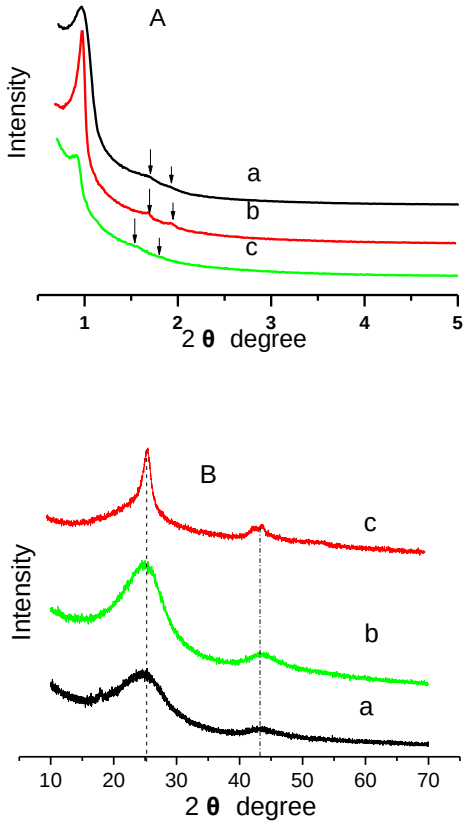

Figure 2 Low-angle (A) and high-angle (B) XRD patterns of N_x/C (a), Co-N_x/C(b) and Fe-N_x/C (c)

The structure, morphology, and textural properties of ordered mesoporous Fe-Nx/C, Co-Nx/C, and Nx/C materials have been analyzed by XRD, TEM, SEM, and N2-sorption techniques. The small-angle X-ray diffraction (XRD) patterns displayed three individual diffraction peaks corresponding to the (100), (110), and (200) reflections the hexagonal structures (Figure 2A), similar to those found in Arranged two-dimensional

mesoporous carbons of the CMK-3 type [36]. Transmission electron microscopy (TEM) images (Figure 3) demonstrated that mesostructures which assembled from rods bonded by smaller subsidiary branches, featuring quasi-cylindrical mesoscale pores with a mean size of approximately 4.0 nm. High-angle XRD patterns showed two peaks at 2θ=25 and 43˚, which correspond to (002) and (101) diffractions of graphitic carbon (Figure 2 B). The d (002) spacing of about 0.36 nm is slightly larger than that of graphite (0.34 nm). Selected-area electron diffraction (SAED) patterns (inset in Figure 3) exhibited clear diffraction rings, indicating the presence of a graphitic phase in the pore walls. High-resolution TEM images (Figure 3 b,d and f) clearly demonstrate the graphitic structure within the mesoporous frameworks of Fe-Nx/C, Co-Nx/C, and Nx/C materials. Unlike the disorganized or semi-crystalline carbon frameworks in prior research on mesoporous Fe-N-C materials [33-35], the well-crystalline graphitic frameworks of Fe-Nx/C, Co-Nx/C, and Nx/C materials are expected to enhance electron conductivity. It should be highlighted that the presence of metal species promotes the crystallization of metal-Nx/C materials, resulting in higher crystallinity compared to Nx/C produced from metal-free pyrolysis of phenanthroline under the same conditions, particularly for Co-Nx/C materials, which exhibit increased (002) diffraction intensity and narrower half-peak widths in C1s XPS peaks [10].

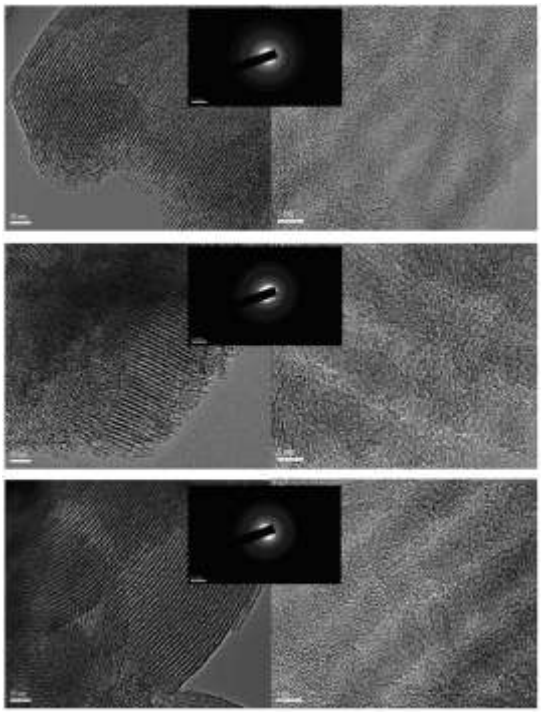

Figure 3 TEM images of Co-Nx/C (a,b), CNx(c,d), and Fe-Nx/C (e,f). Inset is the corresponding SAED image

The developed materials' gas adsorption isotherms (Figure 4A) were analyzed to examine their textural characteristics, all of which display typical IV type curves indicative of mesoporous materials. According to the BJH model derived from desorption tests, the mesopore radius distribution for all samples is centered around 3.8 nm. In comparison to the synthesized Nx/C materials, the Fe-Nx/C (0.70 cm^3/g) and Co-Nx/C (0.56 cm^3/g) showed reduced pore volumes. However, Fe-Nx/C has a BET surface extent (532 m^2/g) that is comparable to that of Nx/C materials, which is greater than that of prior studies on mesoporous Fe-N-C materials produced under inert gas environments [32]. The BET surface extent of Co-Nx/C is inferior to that of both Fe-Nx/C and Nx/C due to its highly graphitic pore walls. These structural and textural property data are sorted in Table 1. The morphologies of the synthesized three materials were also verified through their respective SEM images, which resemble the typical rod-like morphology of SBA-15 materials.

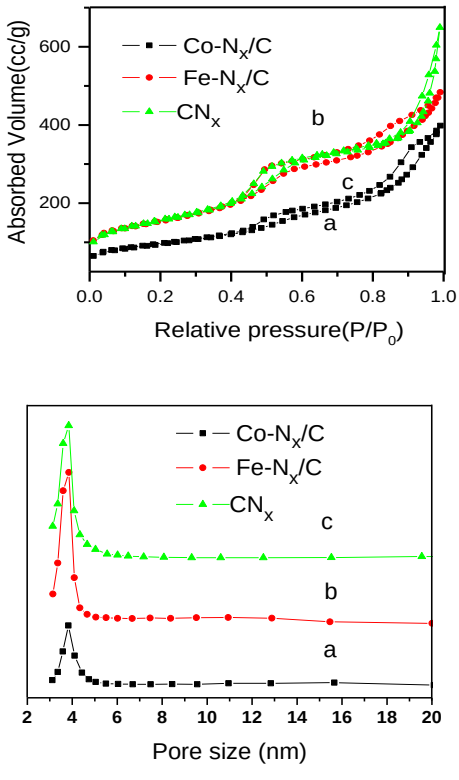

Figure 4 The N_2 sorption isotherms (A) and the corresponding pore size distribution curves (B)

Table 1 The physical and electrochemical parameters of mesoporous materials

Samples	Unit cell parameter (nm)	Surface extent (cm^2/g)	Pore size (nm)	Pore volume (cm^3/g)	Morphology
Co-N_x/C	8.4	330	3.8	0.56	rod
Fe-N_x/C	8.1	532	3.8	0.70	rod
N_x/C	8.1	538	3.8	0.91	rod

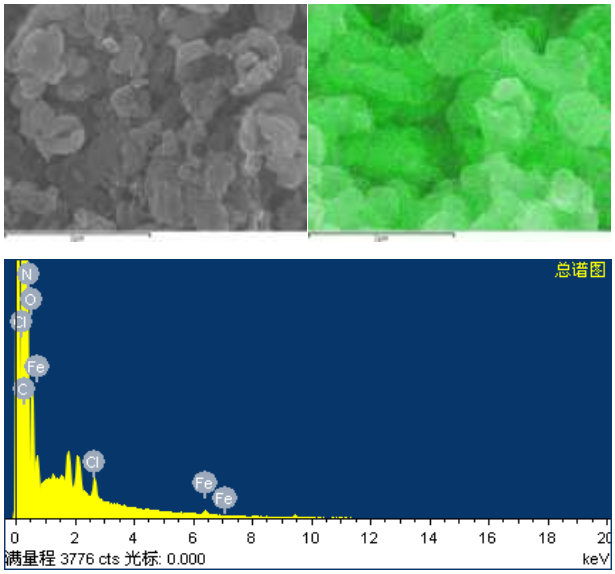

Figure 5 SEM images (A) , SEM-Mapping image(B) and EDS spectrum (C) of ordered mesoporous Fe-N_x/C material

The distribution control for metal and nitrogen active species is very important in the construction of Fe-N_x/C catalytic materials with high activity. The budget-friendly nitrogen precursors such as ethylenediamine, polyaniline, cyanamide, and NH_3do not spontaneously generate uniformly spread Fe-N_x sites prior to pyrolysis. As a result, large Fe or FeCx particles are often inevitably produced during the thermal treatment procedure, which could hinder the building of active sites in the preparation and block the active sites in catalysis. Profiting from the well-Dispersed Fe-N sites prior to pyrolysis in 1,10-phenanthroline iron chelates and the confinement effect of the SBA-15 mesochannels, the presenting Fe-N_x/C materials reveal the well-distributed Fe and N species on carbon frameworks in large domains, illustrated by the EDS-mapping technique. Different from mesoporous Fe-N-C materials prepared by heating formaldehyde resins mixed Fe-N_4 macrocycle molecules [33] and mesoporous CN_x-absorbed iron acetates in NH_3 [34], no any bulk Fe species were observed in this mesostructured Fe-N_x/C material, Consistent with the data of XRD and TEM. In comparison to the previous mesoporous Fe-N-C materials[32-34], the unique Fe-N_x/C materials were expected to facilitate the improving of active site density and the assembling in cathode catalyst layers and promote the rapid diffusion of O_2 molecules.

3.2 Electrocatalytic activity

The electrocatalytic characteristics of mesoporous Fe-Nx/C, Co-Nx/C, and Nx/C substances in a 0.1M KOH alkaline solution were examined using cyclic voltammetry (CV) and rotating disk electrode (RDE) methods. All potentials were referenced against Ag/AgCl, KCl (3 M) in 0.1M KOH for easier comparison. Significant decreases in current were observed as distinct cathodic peaks for all three substances, illustrating considerable electrocatalytic dynamics in oxygen reduction (see Figure 6 A and S3). As illustrated in Figure 6 B and D, the metal–N–C materials showed a significant enhancement in activity compared to mesoporous Nx-C, as evidenced by the notable positive shifts in the ORR cathodic peak potentials for Fe-Nx/C, Co-Nx/C, and Nx-C (-0.11, 0.18, and 0.22V in the CVs, respectively) and their corresponding onset potentials (0.02, -0.08, and -0.1 V in the polar curves at 1600rpm, respectively). Linear regressions based on the Koutecky–Levich equations confirmed that the combination of metal appreciably improved the electron-transfer kinetics (JK) and the measured current densities (J) (Figure 6F), particularly for Fe-Nx/C materials, which reached 16.0 mA cm^{-2} at -0.4V. In contrast to the benchmark Pt-C materials with an onset potential of -0.03V, the onset potential for mesoporous Fe-Nx/C showed a positive shift of 5mV. The JK value for Fe-Nx/C was significantly higher than that of commercial Pt–C (9.6mA cm^{-2}), and the current density (J) of Fe-Nx/C also surpassed that of Pt-C materials in both kinetic and diffusion potential ranges, indicating distinguished electrocatalytic activity for ORR. When contrasted with the highly effective mesoporous CNx developed by Klaus Müllen et al [11], mesoporous Fe-Nx/C exhibited more favorable onset and peak potentials, as well as larger JK and J values under similar measurement conditions, highlighting its enhanced catalytic activity for ORR in 0.1M KOH alkaline media.

The rotating-disk voltammetry profiles for Fe-Nx/C, Co-Nx/C, and Nx/C in O_2-saturated 0.1M KOH indicated that their current densities increased with higher rotation rates (ranging from 400 to 2500 rpm, as shown in Figure 6 C and S4). The Koutecky–Levich (K-L) plots for Fe-Nx/C materials between -0.4 and -0.8 V displayed strong linearity (Figure 6C), implying that the electron transfer numbers for oxygen reduction at various electrode potentials are consistent. The linearity and parallel nature of the plots typically suggest first-order reaction kinetics concerning the concentration of dissolved O_2. Based on the slope of the plots at -0.4V and the Koutecky–Levich equations ($B=0.62nFC_0(D_0)^{2/3}\nu^{1/6}$, $C_0=1.2\times10^{-3}$ mol L^{-1}, $D_0=1.9\times10^{-5}$ cm s^{-1}, $\nu=0.01$ cm^2 s^{-1}), the electron transfer number was turned out to be 4.1, indicating a four-electron transfer process for the mesoporous Fe-Nx/C material during oxygen reduction. In contrast, The incline of the K-L plots for Co-Nx/C and Nx/C between -0.4 and -0.8V differed from one another. The calculated electron transfer numbers at -0.4V were 3.1 for Co-Nx/C and 2.2 for Nx/C, respectively. The electrochemical reduction of O_2 on mesoporous Co-Nx/C involves a interrelation of four-electron and two-electron transfers, while Nx/C primarily follows a two-electron transfer process in the oxygen reduction reaction (ORR). The presence of metal species alters the oxygen reduction pathway for the resulting mesoporous materials, with Fe species promoting a four-electron transfer route.

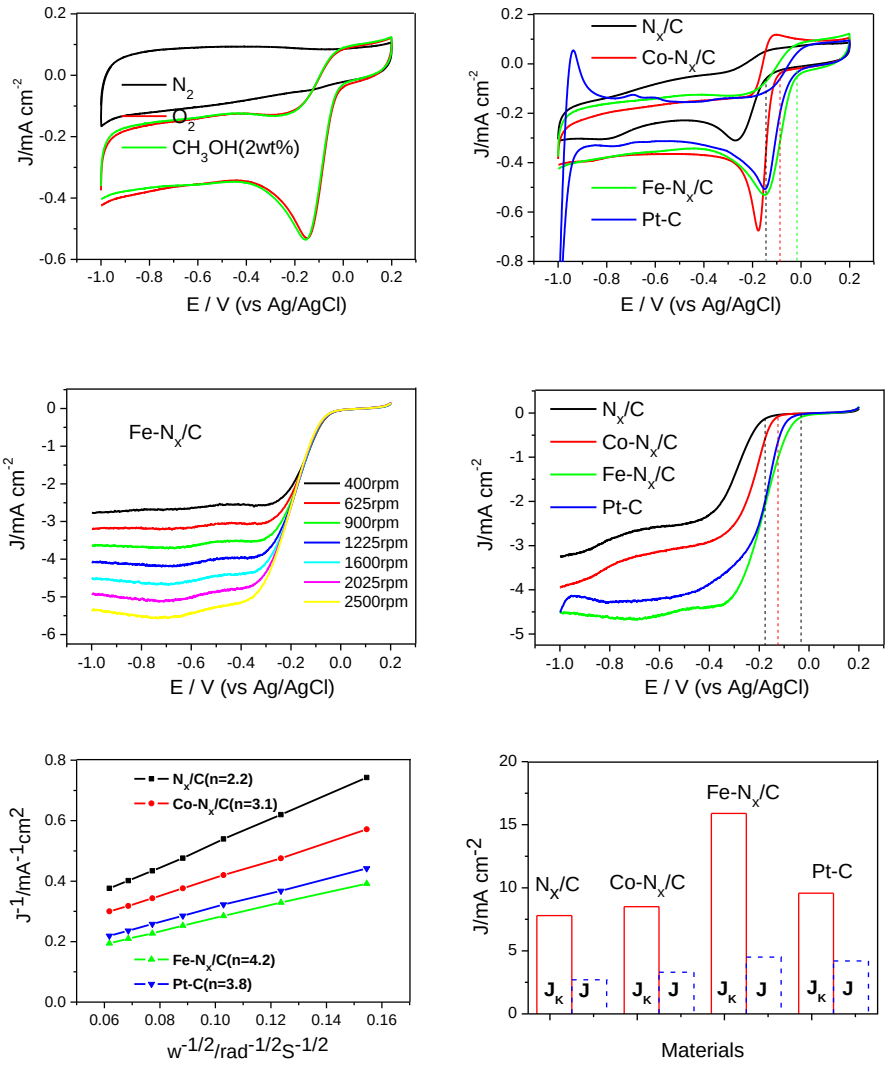

Figure 6 A) Cyclic voltammograms of mesoporous Fe-N_x/C in a 0.1M KOH solution at a scan rate of 10 mV s^{-1}. B) Cyclic voltammograms of diverse mesoporous substances and Pt-C in an O_2-saturated 0.1m solution of KOH at a scan rate of 10 mV s^{-1}. C) Rotating-disk voltammograms documented for mesoporus Fe-N_x/C substances at a range of rotation rates. D) RDE voltammograms of the series of mesoporus substances and Pt-C at a rotation rate of 1600 rpm. E). Koutecky–Levich plot of J_L^{-1} versus ω^{-1} at -0.4V (vs Ag/AgCl) of mesoporus substances and Pt-C at -0.4V(vs Ag/AgCl). F) Electrochemical activity given as the kinetic (J_K)- and diffusion(J_L) limiting current density at -0.4 V (vs Ag/AgCl) for the mesoporus substances and Pt-C.

The electrocatalytic characteristics of Fe-Nx/C, Co-Nx/C, and Nx/C for the oxygen reduction reaction (ORR) in 0.5M H_2SO_4 was examined. All potentials were calibrated against the reversible hydrogen electrode (RHE) in 0.5M H_2SO_4 solutions. The cyclic voltammograms (CVs) of mesoporous Fe-Nx/C and Co-Nx/C in O_2-saturated 0.5M H_2SO_4 showed significant oxygen reduction current peaks at approximately 0.70 and 0.67 V (vs RHE), respectively. In contrast, Nx/C exhibited only a minimal reduction current, suggesting its restricted catalytic efficiency towards the oxygen reduction reaction under acidic environments, consistent with earlier studies. The observed positive shift in the ORR onset potential, extracted from the polar diagrams at 900 rpm, was noted for Fe-Nx/C (0.87 V), Co-Nx/C (0.83 V), and Nx/C (0.70 V), mirroring results found in 0.1M KOH alkaline media. This suggests that mesoporous Fe-Nx/C demonstrates superior catalytic activity in acidic environments.

The onset potential of as-prepared Fe-N_x/C is slightly more negative than that of Pt-C-JM (0.91V) at the catalyst loading of 30ug cm^{-2}. However, it is should be noticed that the escalating catalyst loading of Fe-N_x/C from 30 to 600ug cm^{-2} resulted into the more positive onset-potential and strikingly increasing current density (Figure 7E and table S4), attributing to the superior mass transport ability and expeditious O_2 diffusion in mesoporous materials. The corresponding onset-potential and half-wave potential for the electrode with 600ug cm^{-2} Fe-N_x/C materials are 0.93 and 0.78V in RDE

testing. The difference of half-wave potential between Fe-N_x/C electrode with 600ug cm^{-2} and Pt/C electrode (TKK, 29wt%) with 29 ug Pt cm^{-2} (100ug cm^{-2} Pt-C) determined by polarization curve at 900rpm was only about 3 mV. In contrast, the difference of half-wave potential between PANI-Fe-C materials reported by Edward F. with 600ug cm^{-2} in 0.5M H_2SO_4 and Pt/C(E-TEK, 20wt%) with a loading of 20 ug Pt cm^{-2} in 0.1M $HClO_4$ is 43mV. Moreover, the current density value (2.1mA cm^{-2}) of Fe-N_x/C electrode at 0.8 V determined by polar curves at 900rpm is higher than that of the PANI-Fe-C electrode[29] at the similar testing conditions with 600ug cm^{-2} catalyst loading (about 2.1mA cm^{-2} at 0.8V). This current density value (4.9mA cm^{-2}) of Fe-N_x/C at diffusion region of 0.6V is much higher than the values of Pt-C-JM (3.4mA cm^{-2}), Pt-C-TKK(4.2mA cm^{-2}) and PANI-Fe-C electrode(3.8mA cm^{-2}). Mesoporous Fe-N_x/C materials in testing show the state-of-the-art catalytic activity among the reported NMPCs. In addition, a four electron route in oxygen reduction for Fe-N_x/C is confirmed by the slope of the plots at 0.3V based on of the Koutecky–Levich equations ($B=0.62nFC_0(D_0)^{2/3}\nu^{1/6}$, $C_0=1.13\times10^{-3}$ mol L^{-1}, $D_o=1.83\times10^{-5}$ cm s^{-1}, ν= 0.01 cm^2 s^{-1}) (Figure 7C). The calculated electron number of Co-N_x/C in ORR is 2.5, suggesting a mainly two-process reaction process for ORR. The resultant mesoporous materials with different metal precursors possess the different ORR route in acidic media, similar to the conclusion obtained in alkaline media.

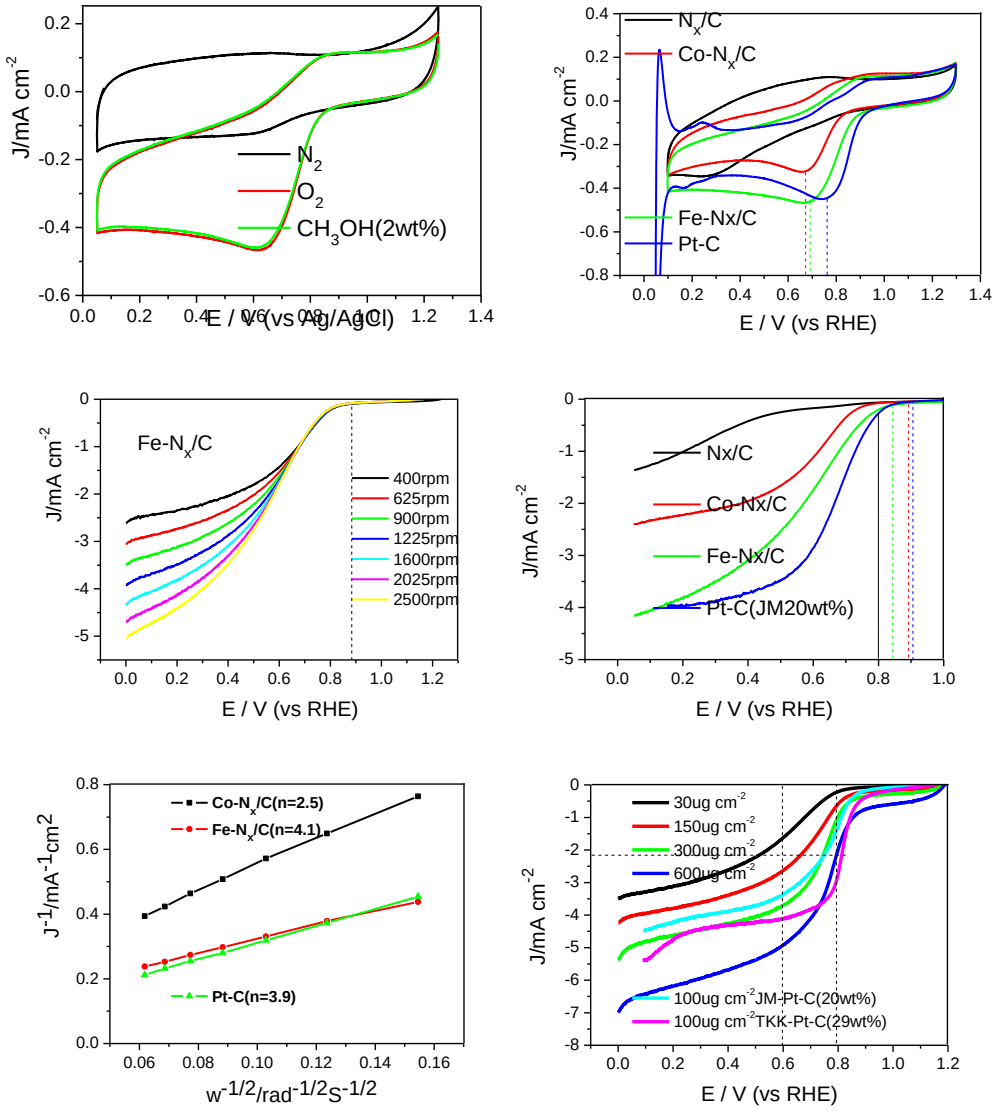

Figure 7 A) Cyclic voltammograms of mesoporous Fe-Nx/C in an O_2-saturated 0.5M solution of H_2SO_4 at a scan rate of 10 mV s^{-1}. B) Cyclic voltammograms of different mesoporous substances and Pt-C in an O_2-saturated 0.5M solution of H_2SO_4 at a scan rate of 10 mV s-1. C) RDE voltammograms of the series of mesoporus substances and Pt-C at a rotation rate of 900 rpm. D) Electrochemical activity given as the kinetic (JK)- and diffusion(JL) limiting current density at 0.0 V (vs RHE) for the mesoporus substances and Pt-C.

3.3 The composition and surface species analysis

As discussed earlier, there was a noticeable increase in catalytic capability for the oxygen reduction reaction (ORR) when comparing Nx/C to Co-Nx/C and Fe-Nx/C in both alkaline and acidic environments. Given their similar mesostructure, morphology, and the higher surface area of Nx/C, the significant discrepancies in ORR activity among these materials can be ascribed to the quantity and type of nitrogen-containing active species present on their surfaces. The nitrogen concentration on the surface layers of these specimens, as measured by X-ray photoelectron spectroscopy (XPS), decreases from Fe-Nx/C (2.6 mol%) to Co-Nx/C (2.1 mol%) and finally to Nx/C (1.7 mol%), which aligns with their decreasing activity. Regarding the types of nitrogen active species, there is a general consensus that nitrogen plays a crucial role.

Table 2 Toutlines the makeup and surface characteristics of mesoporous materials

Samples	C (mol%)	N (mol%)	O (mol%)	Metal[c] (mol%)	N_{N-O} (%)	N_{Pyr} (%)	N_q (%)	N_{N-H} (%)
N_x/C	80.2	1.7	18.1	-	49.8	8.4	18.2	23.6
Co-N_x/C	84.9	2.1	12.6	0.24	15.4	34.0	34.4	16.2
Fe-N_x/C	87.4	2.6	9.8	0.16	12.7	52.7	14.6	19.9

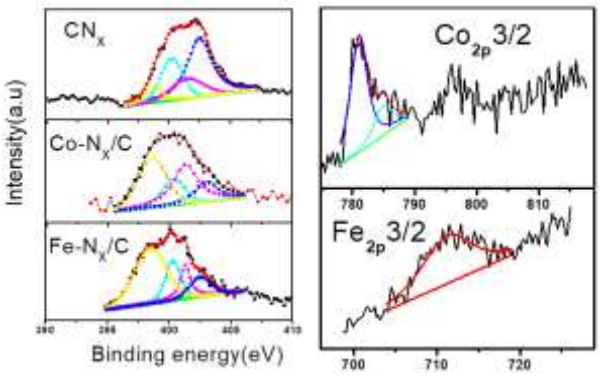

Figure 8 The N1s spectra (B) of Fe-N_x/C, Co-N_x/C and CN_x. (C) is the corresponding $Co_{2p}^{3/2}$ and $Fe_{2p}^{3/2}$ XPS spectra

Incorporating nitrogen into the graphite matrix, particularly for creating pyridine-like nitrogen atoms at the edges of the graphite plane, is essential for developing a highly effective carbon-based catalytic material that is either non-precious metal or metal-free. The nitrogen concentration in Fe-Nx/C, Co-Nx/C, and Nx/C substances was analyzed using N 1s XPS spectra (Figure 8B), which can be broken down into four categories based on binding energy: pyridine-like (398.4 eV), graphite-like (401.3 eV), pyrrollic-like (～400 eV), and pyridine N-oxides (402-404.0 eV). A notable observation is that the metal species in the precursors significantly enhance the amount of pyridine-like nitrogen in M-Nx/C substances, as evidenced by the deconvoluted N1s spectra showing Nx/C (8.4%), Co-Nx/C (34.0%), and Fe-Nx/C (52.7%). Literature suggests that metal species act as catalysts for the formation of pyridine-like nitrogen [38-39]. This study proposes a new role for metal species as protective agents to account for this observation. The proportion of pyridine-N-oxides in the nitrogen species of Co-Nx/C (15.4%) and Fe-Nx/C (12.7%) is significantly lower than that in Nx/C (49.8%), as determined by XPS. The presence of metal ions appears to inhibit the oxidation of pyridine-like nitrogen during pyrolysis, reducing the formation of inactive pyridine-N-oxides in the final products, likely lead to the coordination effect between transition metals and nitrogen.

The role of N-binding metal species and N atoms in CNx as catalytic sites for M-Nx/C catalysts remains a topic of discussion in the literature [1-6]. Our research indicates that mesoporous Nx/C materials exhibit strong catalytic activity in 0.1M KOH alkaline solutions, suggesting that N atoms in carbon, particularly pyridine-N atoms, work as active sites for the oxygen reduction reaction (ORR) in this medium. The enhanced ORR activity observed in Fe-Nx/C and Co-Nx/C can likely be attributed to an increase in pyridine-like nitrogen species on their surfaces. However, the significant difference in ORR activity between mesoporous Fe-Nx/C and Nx/C substances in 0.5M H_2SO_4 acidic solutions is puzzling if N atoms in carbon are the primary active sites, as the mesoporous Nx/C materials still contain approximately 8.4% pyridine-N species on their surface. XPS analysis reveals that Approximately 0.24 mol % Fe and 0.16 mol % Co are present on the external strata of the M-Nx/C materials. The affinity energies of the Fe^{2p} (711.3 eV) and Co^{2p} (781.8 eV) peaks, as determined by XPS, indicate that the predominant metal categories in Fe-Nx/C and Co-Nx/C materials are N-coordinated metals, consistent with earlier research [38,39]. Additionally, pyridine- and pyrrolic-like nitrogen species located at the edges of graphitic structures can also act as metal coordination sites due to their electron-donating characteristics. Therefore, it is believed that both N-binding metal species and N atoms in CNx can serve as active sites for ORR, with M-Nx moieties within the carbon matrix enhancing the catalytic capability of M-Nx/C materials, especially in acidic environments. Overall, the increased surface nitrogen content, particularly with a high proportion of pyridine-like nitrogen and abundant Fe-Nx moieties in the carbon structure, contributes to the exceptional catalytic performance of Fe-Nx/C materials for ORR.

3.4 Methanol-tolerate property and durability

The methanol tolerance of cathode catalysts is a significant issue in direct-methanol fuel cells. To investigate potential crossover effects, we assessed the electrocatalytic selectivity of mesoporous Fe-Nx/C and Pt-C-JM in O_2-saturated 0.1M KOH with 2wt% methanol. In the CV curve for Pt-C-JM, we observed two peaks at -0.35 and -0.20 V (vs Ag/AgCl) corresponding to methanol oxidation,

while the cathodic current maximum for the oxygen reduction reaction (ORR) disappeared. In contrast, mesoporous Fe-Nx/C showed no significant change in the oxygen-reduction current under the same conditions (Figure 6 A). Similar results were noted for both mesoporous Fe-Nx/C and Pt-C-JM in 0.5M H_2SO_4, where the addition of 2wt% CH_3OH in O_2-saturated 0.5M H_2SO_4 had minimal impact on the oxygen reduction current peak and onset potential of Fe-Nx/C in CV measurements (Figure 7A). Additionally, we tested the durability of Fe-Nx/C materials at a constant voltage for 20,000 seconds in O_2-saturated 0.1M KOH or 0.5M H_2SO_4 solutions at a turning velocity of 1600 rpm (Figure 9). The current-time (i-t) chronoamperometric response of Fe-Nx/C showed a relatively moderate reduction, maintaining a significant relative current of 74% in 0.1M KOH and 76% in 0.5M H_2SO_4 after 20,000 seconds. In comparison, the Pt-C-JM electrode with the same catalyst loading (30 μg cm^{-2}) exhibited a current drop to about 58.0% in 0.1M KOH and 50% in 0.5M H_2SO_4 after 20,000 seconds. Overall, the durability and selectivity of Fe-Nx/C materials for ORR outperform those of the Pt-C-JM catalyst in both alkaline and acidic environments.

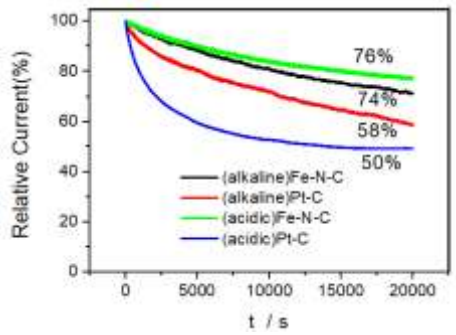

Figure 9 Current–time (i–t) chronoamperometric response of mesoporus Fe-Nx/C and Pt–C (JM, 20wt%) at -0.4 V(vs Ag/AgCl) in O_2-saturated 0.1mKOH at a rotation rate of 1600 rpm (A) and at 0.25 V(vs RHE) in O_2-saturated 0.5M H_2SO_4 at a rotation rate of 1600 rpm with the catalyst loading of 30ug cm^{-2}

4 Conclusions

In conclusion, we have successfully constructed an ordered mesoporous Fe-N_x/C materials with outstanding ORR performance by a novel metal chelate pyrolysis nanocasting approach using low-cost Fe phenanthroline chelates as the precursors. As compared to customary Pt-C catalysts and the reported NPMCs, this novel self-supporting catalyst exhibits the conspicuous ORR catalytic activity in term of the ORR current density and onset potential in both alkaline media and acidic media. The ordered mesostructure with high surface area, nitrogen-enriched graphitic backbones, and the abundant pyridine-like nitrogen and Fe-N_x moieties within carbons contributed to the excellent catalytic activity of Fe-N_x/C for ORR. The mesoporous Fe-N_x/C materials prepared by this novel synthesis method may be used as the practically promising substitute for the expensive noble metal catalysts in PEMFCs.

Fund Projects: The author gratefully acknowledges financial support from the Research project of Hebei Normal University for nationalities (No. STZD2023001) and Research on the Key Technologies for Collaborative Development of Clean Energy Development and Ecological Protection in Chengde (No. 202305B100); Research project of Hebei Minzu Normal University (No. DR2023001).

References

[1] A. Brouzgou, S.Q. Song, Panagiotis E. Tsiakaras. Low and non-platinum electrocatalysts for PEMFCs: Current status, challenges and prospects [J]. Applied Catalysis B: Environmental, 2012(127):371–388.

[2] Rapidah Othman, Andrew L. Dicks, Zhonghua Zhu. Non precious metal catalysts for the PEM fuel cell cathode [J]. international journal of hydrogen energy, 2012(37):357-372.

[3] Cicero W. B. Bezerra, Lei Zhang, Kunchan Lee, et,al. A review of Fe-N/C and Co-N/C catalysts for the oxygen reduction reaction [J]. Electrochimica Acta, 2008(53):4937–4951.

[4] Adina Morozan, Bruno Jousselme and Serge Palacin. Electrochemical performance of annealed cobalt – benzotriazole/CNTs catalysts towards the oxygen reduction reaction [J]. Energy & Environmental Science, 2011(4):1238–1254.

[5] Zhongwei Chen, Drew Higgins, Aiping Yu, et,al. A review on non-precious metal electrocatalysts for PEM fuel cells [J]. Energy & Environmental Science, 2011(4):3167–3192.

[6] Frédéric Jaouen, Eric Proietti, Michel Lefèvre, et al. Recent advances in non-precious metal catalysis for oxygen-reduction reaction in polymer electrolyte fuel cells [J]. Energy & Environmental Science, 2011,4(1):114-130.

[7] Kuanping Gong, Feng Du, Zhenhai Xia, et al. Nitrogen-doped carbon nanotube arrays with high electrocatalytic activity for oxygen reduction[J]. science, 2009,323(5915):760-764.

[8] Zhijian Wang, Rongrong Jia, Jianfeng Zheng, et al. Nitrogen-promoted self-assembly of N-doped carbon nanotubes and their intrinsic catalysis for oxygen reduction in fuel cells[J]. Acs Nano, 2011,5(3):1677-1684.

[9] Liangti Qu, Yong Liu, Jong-Beom Baek, et al. Nitrogen-doped graphene as efficient metal-free electrocatalyst for oxygen reduction in fuel cells [J]. ACS nano, 2010,4(3):1321-1326.

[10] Ziyin Lin, Min-kyu Song, Yong Ding, et al. Facile preparation of nitrogen-doped graphene as a metal-free catalyst for oxygen reduction reaction [J]. Physical Chemistry Chemical Physics, 2012,14(10):3381-3387.

[11] Ruili Liu, Dongqing Wu, Xinliang Feng, et al. Nitrogen-doped ordered mesoporous graphitic arrays with high electrocatalytic activity for oxygen reduction [J]. Angewandte Chemie International Edition, 2010,14(49):2565-2569.

[12] Wen Yang, Tim-Patrick Fellinger, and Markus Antonietti. Efficient metal-free oxygen reduction in alkaline medium on high-surface-area mesoporous nitrogen-doped carbons

made from ionic liquids and nucleobases [J]. Journal of the American Chemical Society, 2011,133(2):206-209.
[13] Xiqing Wang, Je Seung Lee, Qing Zhu, et al. Ammonia-treated ordered mesoporous carbons as catalytic materials for oxygen reduction reaction [J]. Chemistry of Materials, 2010,22(7):2178-2180.
[14] Ki Rak Lee, Kye Ung Lee, Jong Wook Lee, et al. Electrochemical oxygen reduction on nitrogen doped graphene sheets in acid media[J]. Electrochemistry Communications, 2010,12(8):1052-1055.
[15] Dingshan Yu, Qiang Zhang, Liming Dai, Highly efficient metal-free growth of nitrogen-doped single-walled carbon nanotubes on plasma-etched substrates for oxygen reduction [J]. Journal of the American Chemical Society, 2010,132(43):15127-15129.
[16] Michel Lefèvre, Eric Proietti, Frédéric Jaouen, et al. Iron-based catalysts with improved oxygen reduction activity in polymer electrolyte fuel cells [J]. science, 2009,324(5923):71-74.
[17] Hansan Liu, Zheng Shi, Jianlu Zhang, et al. Ultrasonic spray pyrolyzed iron-polypyrrole mesoporous spheres for fuel celloxygen reduction electrocatalysts [J]. Journal of Materials Chemistry, 2009,19(4):468-470.
[18] Thorsten Schillinga, Michael Bronb, Oxygen reduction at Fe–N-modified multi-walled carbon nanotubes in acidic electrolyte [J]. Electrochimica Acta, 2008,53(16):5379-5385.
[19] Robert L. Arechederra, Kateryna Artyushkova, Plamen Atanassov, et al. Growth of phthalocyanine doped and undoped nanotubes using mild synthesis conditions for development of novel oxygen reduction catalysts [J]. ACS applied materials & interfaces, 2010,2(11):3295-3302.
[20] Ulrike I. Koslowski, Irmgard Abs-Wurmbach, Sebastian Fiechter, et al. Nature of the catalytic centers of porphyrin-based electrocatalysts for the ORR: a correlation of kinetic current density with the site density of Fe− N4 centers [J]. The Journal of Physical Chemistry C, 2008,112(39):15356-15366.
[21] Médard C., Lefèvre M., Dodelet J. P., et al. Oxygen reduction by Fe-based catalysts in PEM fuel cell conditions: activity and selectivity of the catalysts obtained with two Fe precursors and various carbon supports [J]. Electrochimica Acta, 2006,51(16):3202-3213.
[22] Xin Wang, Wenzhen Li, Zhongwei Chen, et al. Durability investigation of carbon nanotube as catalyst support for proton exchange membrane fuel cell [J]. Journal of Power Sources, 2006,158(1):154-159.
[23] Cicero W. B. Bezerra,Lei Zhang,Kunchan Lee, et al. Novel carbon-supported Fe-N electrocatalysts synthesized through heat treatment of iron tripyridyl triazine complexes for the PEM fuel cell oxygen reduction reaction [J]. Electrochimica Acta, 2008,53(26):7703-7710.
[24] Hansan Liu, Zheng Shi, Jianlu Zhang, et al. Ultrasonic spray pyrolyzed iron-polypyrrole mesoporous spheres for fuel celloxygen reduction electrocatalysts [J]. Journal of Materials Chemistry, 2009,19(4):468-470.
[25] Ja-Yeon Choi, Drew Higgins, Zhongwei Chen. Highly durable graphene nanosheet supported iron catalyst for oxygen reduction reaction in PEM fuel cells [J]. Journal of the Electrochemical Society, 2011,159(1):B86−B90.
[26] Ja-Yeon Choi, Ryan Hsu, Zhongwei Chen. Nanoporous carbon-supported Fe/Co-N electrocatalyst for oxygen reduction reaction in PEM fuel cells [J]. ECS Transactions, 2010,28(23):101-112.
[27] Ja-Yeon Choi, Ryan S. Hsu, Zhongwei Chen. Highly active porous carbon-supported nonprecious metal− N electrocatalyst for oxygen reduction reaction in PEM fuel cells [J]. The Journal of Physical Chemistry C, 2010,114(17):8048-8053.
[28] Ryan S. Hsu, Zhongwei Chen. Improved Synthesis Method for a Cyanamide Derived Non-Precious ORR Catalyst for PEFCs [J]. ECS Transactions, 2010,28(23):39−46.
[29] Edward F. Holby, Gang Wu, Piotr Zelenay, et al. Structure of Fe-Nx-C defects in oxygen reduction reaction catalysts from first-principles modeling [J]. The Journal of Physical Chemistry C, 2014,118(26):14388-14393.
[30] Shayna Brocato, Alexey Serov, Plamen Atanassov, pH dependence of catalytic activity for ORR of the non-PGM catalyst derived from heat-treated Fe–phenanthroline [J]. Electrochimica acta, 2013(87):361-365.
[31] Xiufang Chen, Young-Si Jun, Kazuhiro Takanabe, et al. Ordered mesoporous SBA-15 type graphitic carbon nitride: a semiconductor host structure for photocatalytic hydrogen evolution with visible light [J]. Chemistry of Materials, 2009,21(18):4093-4095.
[32] Lei M., Li P. G., Li. L. H., et al. A highly ordered Fe-N-C nanoarray as a non-precious oxygen-reduction catalyst for proton exchange membrane fuel cells [J]. Journal of Power Sources, 2011,196(7):3548-3552.
[33] Gang Liu, Xuguang Li, Prabhu Ganesan, et al. Development of non-precious metal oxygen-reduction catalysts for PEM fuel cells based on N-doped ordered porous carbon [J]. Applied Catalysis B: Environmental, 2009,93(1-2):156-165.
[34] Xu J. B., Zhao* T. S., Zeng L. Covalent hybrid of hemin and mesoporous carbon as a high performance electrocatalyst for oxygen reduction [J]. international journal of hydrogen energy, 2012,37(21):15976-15982.
[35] Shinae Jun, Sang Hoon Joo, Ryong Ryoo, et al. Synthesis of new, nanoporous carbon with hexagonally ordered mesostructure [J]. Journal of the American chemical society, 2000,122(43):10712-10713.
[36] Yuta Nabae, Shogo Moriya, Katsuyuki Matsubayashi, et al. The role of Fe species in the pyrolysis of Fe phthalocyanine and phenolic resin for preparation of carbon-based cathode catalysts [J]. CARBON, 2010(10):2613-2624.
[37] Maldonado, Stephen, Keith J. Stevenson. Influence of Nitrogen Doping on Oxygen Reduction Electrocatalysis at Carbon Nanofiber Electrodes [J]. The Journal of Physical Chemistry B,2005,109(10):4707-4716.
[38] Nalini P. Subramanian, Xuguang Li, Vijayadurda Nallathambi, et al. Nitrogen-modified carbon-based catalysts for oxygen reduction reaction in polymer electrolyte membrane fuel cells [J]. Journal of Power Sources, 2009,188(1):38-44.
[39] Vijayadurga Nallathambi, Jong-Won Lee, Swaminatha P. Kumaraguru, et al. Development of high performance carbon composite catalyst for oxygen reduction reaction in PEM Proton Exchange Membrane fuel cells [J]. Journal of Power Sources, 2008,183(1):34-42.